

CHAPTER III

THEORY



3.1 Zeolites

Zeolites were first identified by Constredt in 1756 [26]. The word 'Zeolite', from the Greek words meaning "boiling stones", alludes to the frothing and bubbling observed by Contredt when he heated several crystals.

Zeolites are finding applications in many areas of catalysis, generating interest in these materials in industrial and academic laboratories. As catalyst, zeolites exhibit appreciable acid activity with shape-selectivity features not available in the compositional equivalent amorphous catalysts. In addition, these materials can act as supports for numerous catalytically active metals. Major advances have occurred in the synthesis of zeolites since the initial discovery of the synthetic zeolite's type A, X and Y, and a great number of techniques have evolved for identifying and characterizing these materials. Added to an extensive and ever growing list of aluminosilicate zeolites are molecular sieves containing other elemental compositions. These materials differ in their catalytic activity relative to the aluminosilicate zeolites and may have potential in customizing or tailoring the molecular sieves catalyst for specific applications. Elements isoelectronic with Al^{+3} or Si^{+4} have been proposed to substitute into the framework lattice during synthesis. These include B^{+3} , Ga^{+3} , Fe^{+3} , and Cr^{+3} substituting for Al^{+3} , and Ge^{+4} and Ti^{+4} for Si^{+4} . The incorporation of transition elements such as Fe^{+3} for

framework Al^{+3} positions modifies the acid activity and, in addition, provides a novel means of obtaining high dispersions of these metals within the constrained pores of industrially interesting catalyst materials.

3.1.1 Structure of Zeolite

Zeolites are porous, crystalline aluminosilicates that develop uniform pore structure having minimum channel diameter of 0.3-0.1 nm. This size depends primarily upon the type of zeolites. Zeolites provide high activity and unusual selectivity in a variety of acid-catalyzed reactions. Most of the reactions are caused by the acidic nature of zeolites.

The structure of zeolite consists of a three-dimensional framework of SiO_4 or AlO_4 tetrahedra, each of which contains a silicon or aluminum atom in the center (Figure 3.1). The oxygen atoms are shared between adjoining tetrahedra, which can be present in various ratios and arranged in a variety of way. The framework thus obtained contains pores, channels, and cages, or interconnected voids.

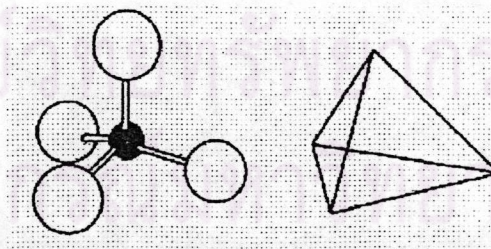


Figure 3.1 SiO_4 or AlO_4 tetrahedra [26].

A secondary building unit (SBU) consists of selected geometric groupings of those tetrahedra. There are nine such building units, which can be used to describe all of known zeolite structures. These secondary building units consist of 4(S4R),

6(S6R), and 8(S8R)-member single ring, 4-4(D4R), 6-6(D6R), 8-8(D8R)-member double rings, and 4-1, 5-1, and 4-4-1 branched rings[27]. The topologies of these units are shown in Figure 3.2. Also listed are the symbols used to describe them. Most zeolite framework can be generated from several different SBU's. Descriptions of known zeolite structures based on their SBU's are listed in Table 3.1[27]. Both zeolite ZSM-5 and ferrierite are described by their 5-1 building units. Offretite, zeolite L, cancrinite, and erionite are generated using only single 6-member rings. Some zeolite structures can be described by several building units. The sodalite framework can be built from either the single 6-member ring or the single 4-member ring. Faujasite (type X or type Y) and zeolite A can be constructed using 4 ring or 6 ring building units. Zeolite A can also be formed using double 4 ring building units, whereas faujasite cannot.

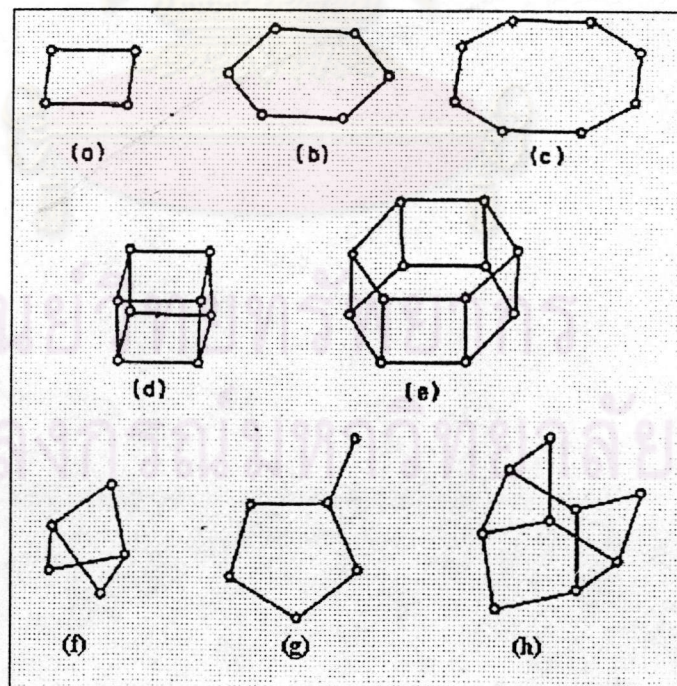
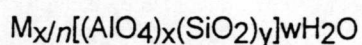


Figure 3.2 Secondary building units (SBU's) found in zeolite structures [51].

Zeolites may be represented by the general formula,



where the term in brackets is the crystallographic unit cell. The metal cation of valence n is present to produce electrical neutrality since for each aluminum tetrahedron in the lattice there is an overall charge of -1 [28]. M is a proton, the zeolite becomes a strong Bronsted acid. As catalyst, zeolite becomes a strong Bronsted acid. As catalysts, zeolites are unique in their ability to discriminate between reactant molecular size and shape [30].

The catalytically most significant are those having pore openings characterized by 8-, 10-, and 12- rings of oxygen atoms. Some typical pore geometries are shown in figure 3.3 [31].

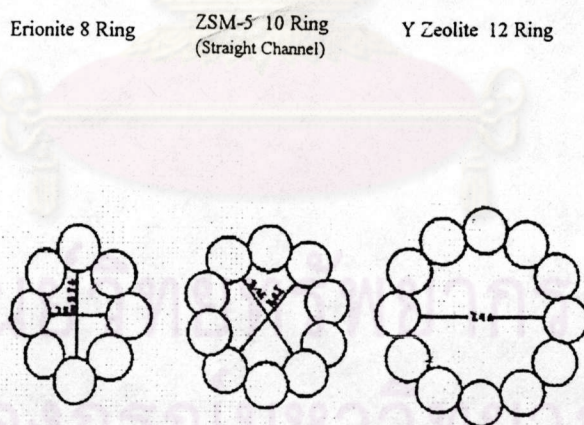


Figure 3.3 Typical Zeolite pore geometries [31].

Table 3.1 Zeolites and their secondary building units. The nomenclature used is consistent with that presented in Figure 3.2 [27].

ZEOLITE	SECONDARY BUILDING UNITS								
	4	6	8	4-4	6-6	8-8	4-1	5-1	4-4-1
Bikitaite								X	
Li-A (BW)	X	X	X						
Analcime	X	X							
Yugawaralite	X		X						
Episitbite								X	
ZSM-5								X	
ZSM-11								X	
Ferrierite								X	
Dachiardite								X	
Brewsterite	X								
Laumonite		X							
Mordenite								X	
Sodalite	X	X							
Henulandite									X
Stibite									X
Natrolite							X		
Thomsonite							X		
Edingtonite							X		
Cancrinite		X							
Zeolite L		X							
Mazzite	X								
Merlinoite	X		X			X			
Phillipsite	X		X						
Zeolite Losod		X							
Erionite	X	X							
Paulingite	X								
Offretite		X							
TMA-E (AB)	X	X							
Gismondine	X		X						
Levyne		X							
ZK-5	X	X	X		X				
Chabazite	X	X			X				
Gmelinite	X	X	X		X				
Rho	X	X	X			X			
Type A	X	X	X	X					
Faujasite	X	X			X				

3.1.1.1 Small pore zeolites

Structures of some of small pore zeolite are illustrated in Figure 3.4. The erionite structure, Figure 3.4(a), is hexagonal containing "supercage" supported by columns of cancrinite units linked through double 6 rings. Access to, and between, the supercages is gained through 8 rings.

In the chabazite framework, Figure 3.4(b), the double 6 rings layer sequence is ABCABC, and the double 6 ring units are linked together through tilted 4 ring units. The framework contains large ellipsoidal cavities, Figure 3.3(c), each entered through six 8 ring units. These cavities are joined together via their 8 ring units, forming a 3 dimensional channel system.

3.1.1.2 Medium pore zeolites

The channel system of zeolite ZSM-5, represented in Figure 3.5, consists of straight channels running parallel to [010] and intersecting sinusoidal channels parallel to [100]. The channels are ellipsoidal with 10 oxygen ring opening, having the approximate free dimensions $5.4 \times 5.6 \text{ \AA}$ (straight channel) and $5.1 \times 5.4 \text{ \AA}$ (sinusoidal channel) based on oxygen radii 1.35 \AA .

3.1.1.3 Large pore zeolites

The faujasite structure, Figure 3.6(a), is built up of truncated octahedra interconnected via double 6 ring units. Faujasite contains extremely large supercages ($\sim 13 \text{ \AA}$ diameter) entered through 12 oxygen ring.

Mordenite, Figure 3.6(b), is characterized by a one dimensional system of parallel elliptical channels, defined by 12 oxygen ring.

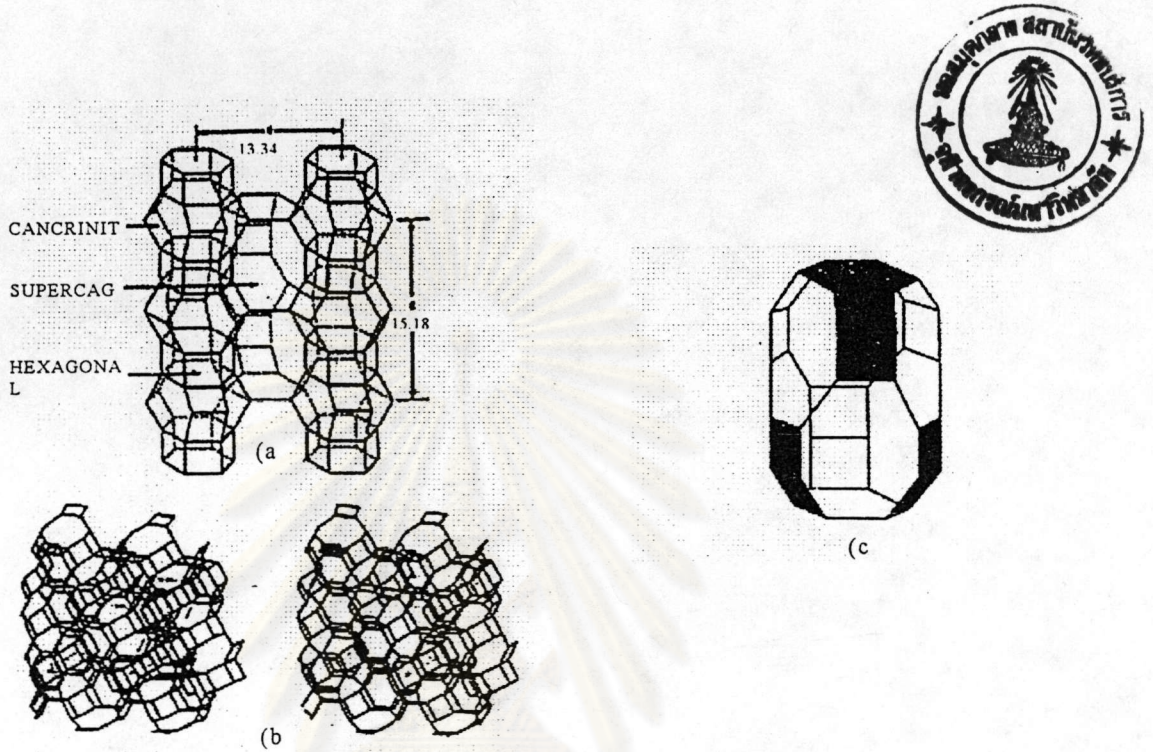


Figure 3.4 Small pore zeolites (a) Erionite framework (b) Chabazite framework (c) Chabazite cavity [31].

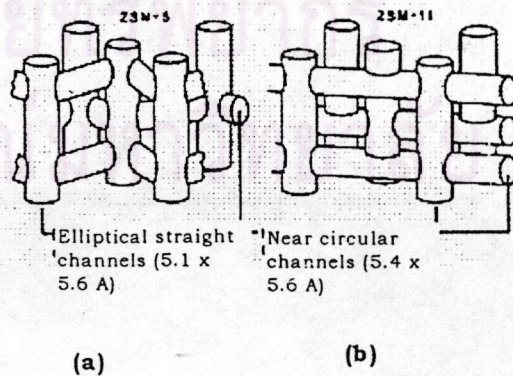


Figure 3.5 ZSM-5 and ZSM-11 channel system [31].

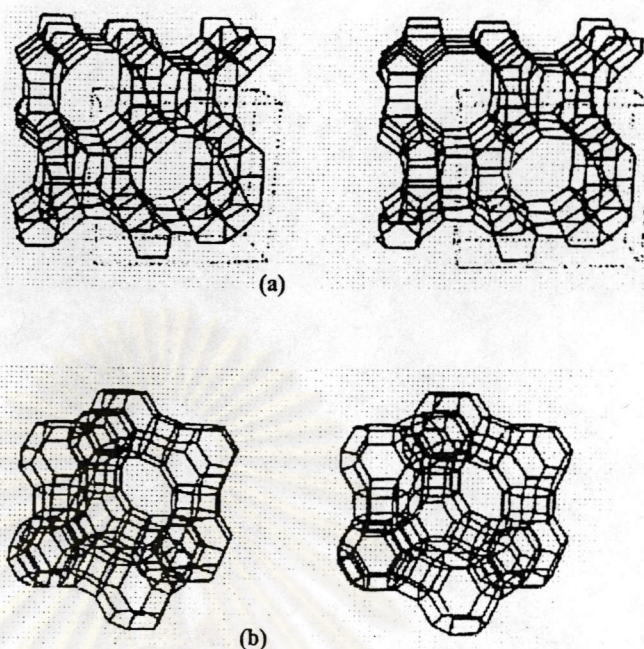


Figure 3.6 Large pore zeolites

(a) Mordenite framework

(b) Faujasite framework [31].

3.1.2 Silicalite and ZSM-5

In silicalite and ZSM-5, the tetrahedra are linked to form the chain-type building block in Figure 3.7. The chain can be connected to form a layer, as shown in Figure 3.8. Rings consisting of five O atoms are evident in this structure; the name *pentasil* is therefore used to describe it. Also evident in Figure 3.8 are rings consisting of 10 oxygen atoms; these are important because they provide opening in the structure large enough for passage of even rather large molecules. The layers can be linked in two ways, the neighboring layers being related either by the operation of a mirror or an inversion. The former pertains to the zeolite ZSM-11, the later to silicalite or ZSM-5, intermediate structures constitute the pentasil series.

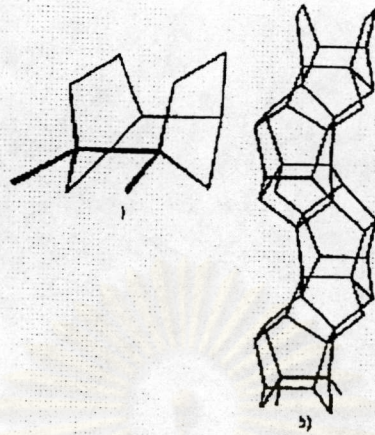


Figure 3.7 The chain-type building block formed from the secondary building units [32].

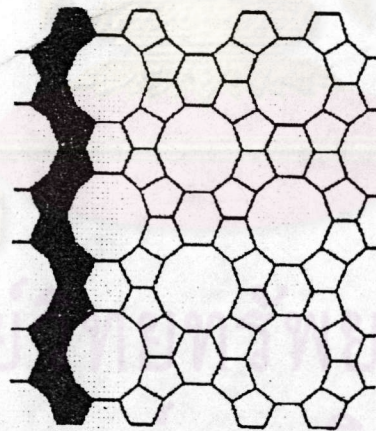


Figure 3.8 Schematic diagram of silicalite layers [32].

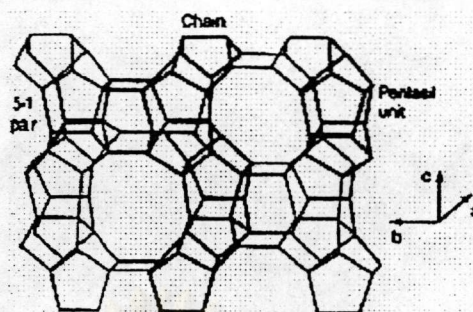


Figure 3.9 Three dimensional structure of silicalite (ZSM-5)[32].

The three dimensional structure of silicalite (and ZSM-5) is presented in Figure 3.9. The 10-membered rings provide access to a network of intersecting pores within the crystal. The pore structure is depicted schematically in Figure 3.5; there is a set of straight, parallel pores intersected by set of perpendicular zigzag pores. Many molecules are small enough to penetrate into this intracrystalline pore structure, where they may be catalytically converted.

3.2 Zeolites as Catalysts [26]

The first use of zeolite as catalysts occurred in 1959 when zeolite Y was used as an isomerization catalyst by Union Carbide. More important was the first use of zeolite X as a cracking catalyst in 1962, based upon earlier work by Plank and Rosinski. They noted that relatively small amounts of zeolites could usefully be incorporated into the then-standard silica/alumina or silica/clay catalysts. The use of zeolite in this way as promoters for petroleum cracking greatly improved their performance.



3.2.1 Potential versatility of zeolites as catalysts

Vaughan has graphically described zeolites as 'molecules boxes' which have variable dimensions suited to the encouragement of molecular rearrangements inside their confined geometry. The conditions inside the 'box', and of the 'box' itself, can be controlled in a variety of ways based upon the unique properties of zeolite frameworks as summarized in Table 3.2 and described below.

Table 3.2 Correlation between zeolite properties and catalytic functionality [26].

Property	Catalytic functionality
Crystal voidage and channels	Extensive internal surface to encourage catalytic processes
Variable pore size	Creates both reactant and product selectivity via molecules sieving
Ion exchange	Cations (i) control pore size, (ii) create high potential energy fields within voidage (active sites) and (iii) enable distribution of catalytically active metals on the zeolite substrate
Salt occlusion	Controls pore size, provide another method of metal incorporation and can improve thermal stability and poisoning resistance
Framework modification	Varies lattice charge (by synthesis or modification) to enhance active site production and thermal stability

3.2.1.1 Crystal voidage and channels

Although some heterogeneous reactions will take place at the external crystal surfaces, most practical zeolite catalysis takes place inside the framework. Here zeolites have the advantage of a very large internal surface, about 20 times

larger than their external surface for the more open framework (e.g. zeolites X and Y). This internal capacity provides the appropriate surfaces at which catalytic transformations can take place. In the faujasite zeolites this is typically in the series of large cavities easily available via three-dimensional open-pore networks.

Further flexibility which is useful for planned catalytic uses arises in the more recently produced zeolites with subtly different cavity and channel systems. ZSM-5, for instance, has a three-dimensional system linked via intersections rather than cavities and mordenite catalysis seems to take place only in the largest channels.

3.2.1.2 Variable pore sizes

Given that catalysis take place largely within zeolite frameworks, access to this environment is patently controlled by oxygen windows. This is diffusion limited process, as is the egress of product molecules after transformations have taken place. This means that zeolites have very special practical advantages over the more traditional catalysts, in that they will admit only certain reactant molecules and that this can be potentially tailored to produced selected products. This selectivity is known as 'shape-selective catalysis' and controlled by 'configurational diffusion' -this phrase was coined by Weiss to express a diffusion regime in which useful catalytic reactions and promoted by virtue of a matching of size, shape and orientation of the reactant product molecules to the geometry of zeolitic framework.

3.2.1.3 Ion exchange

Perhaps more relevant is the way in which ion exchange can be employed to place cations into very specific framework sites so as to create small volumes of high electrostatic field. These fields are 'active sites' to which an organic reactant molecule can be attracted thus promoting the bond distortion and rupture essential to molecular rearrangements.

Another feature of ion exchange is that it provides a route for the introduction of metal cations with a view to their subsequent reduction to metal particles. These exist in the so-called 'bifunctional' zeolite catalysts used to effect both hydrogenation and dehydrogenation reactions.

3.2.1.4 Salt occlusion

The introduction of a salt molecule into a zeolite can be the first stage in the incorporation of a metal for subsequent reduction as mentioned above. It can also be used to enhance thermal stability. Yet another purpose is to 'pacify' zeolite cracking catalysts. The problem here is that crude oils contain metal cations (Ni, Cu, V, Fe) originating from the metal porphyrins thought to play an inherent part in the geological formation of oil. These metals create unwanted reactivity causing carbon (coke) formation and subsequent loss of catalytic properties. The occlusive introduction of stannates, bismuthates, or antimonates pacifies these metals to extend useful catalyst bed life. It enables the refinery to cope with a variety of crude oils from

different oil fields and illustrates the flexible technology which can be achieved in zeolite catalysis.

Other salt treatments, via phosphates or fluorides, have been used to improve performance.

3.2.1.5 Framework modification

The electrostatic field a zeolite can be manipulated by isomorphous substitution into framework Si and Al sites. This can be done by synthetic or modification routes. When the Si : Al ratio is close to 1 the field strength is at its highest as is the cation content - i.e. the conditions of maximum negative charge on the framework. An increase of the Si:Al causes a greater separation of negative charge and hence higher field gradients (obviously also conditioned by cation position and cation type). In this way catalytic activity can be controlled, and other parameters altered. A well - known example of these effects is the way in which the thermal and chemical stabilities of the synthetic faujasites can be critically altered by aluminium removal.

Framework substitution also can be created by the introduction of atoms other than Si and Al into tetrahedral sites via synthesis or modification. ZSM-5 can accept B and Ga into tetrahedral sites by simple salt treatment as mentioned earlier, although a similar reaction in other frameworks is by no means as facile.

3.3 Zeolite Active Sites

3.3.1 Acid Sites

Classical Bronsted and Lewis acid models of acidity have been used to classify the active sites on zeolites. Bronsted acidity is proton donor acidity; a tridiagonally co-ordinated alumina atom is an electron deficient and can accept an electron pair, therefore behaves as a Lewis acid [30, 33].

In general, the increase in Si/Al ratio will increase acidic strength and thermal stability of zeolite [34]. Since the number of acidic OH groups depend on the number of aluminum in zeolite's framework, decrease in Al content is expected to reduce catalytic activity of zeolite. If the effect of increase in the acidic centers, increase in Al content, shall result in enhancement of catalytic activity.

Based on electrostatic consideration, the charge density at a cation site increases with increasing Si/Al ratio. It was conceived that these phenomena are related to reduction of electrostatic interaction between framework sites, and possibly to difference in the order of aluminum in zeolite crystal - the location of Al in crystal structure [33].

Recently it has been reported the mean charge on the proton was shifted regularly towards higher values as the Al content decreased [30]. Simultaneously the total number of acidic hydroxyls, governed by the Al atoms, were decreased. This evidence emphasized that the entire acid

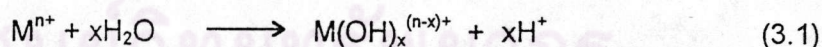
strength distribution (weak, medium, strong) was shifted towards stronger values. That is, weaker acid sites become stronger with the decrease in Al content.

An improvement in thermal or hydrothermal stability has been ascribed to the lower density of hydroxyls groups which is parallel to that of Al content [30]. A longer distance between hydroxyl groups decreases the probability of dehydroxylation that generates defects on structure of zeolites.

3.3.2 Generation of Acid Centers

Protonic acid centers of zeolite are generated in various ways. Figure 3.10 depicts the thermal decomposition of ammonium exchanged zeolites yielding the hydrogen form [27].

The Bronsted acidity due to water ionization on polyvalent cations, described below, is depicted in figure 3.11 [28].



The exchange of monovalent ions by polyvalent cations could improve the catalytic property. Those highly charged cations create very acidic centers by hydrolysis phenomena.

Bronsted acid sites are also generated by the reduction of transition metal cations. The concentration of OH groups of zeolite containing transition metals

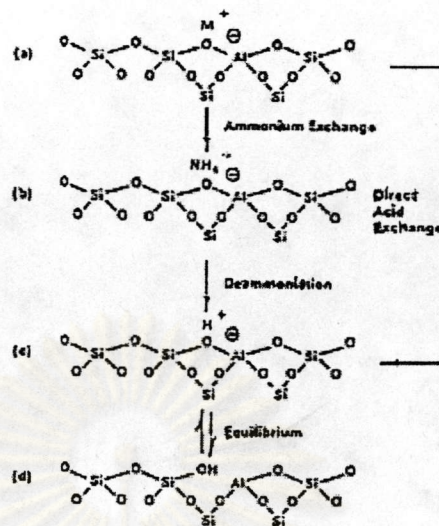


Figure 3.10 Diagram of the surface of a zeolite framework [27].

- In the as-synthesized form M^+ is either an organic cation or an alkali metal cation.
- Ammonium in exchange produces the NH_4^+ exchanged form.
- Thermal treatment is used to remove ammonia, producing the H^+ , acid, form.
- The acid form in (c) is in equilibrium with the form shown in (d), where there is a silanol group adjacent to a tricoordinate aluminum.

ศูนย์วิจัยทรัพยากร
จุฬาลงกรณ์มหาวิทยาลัย

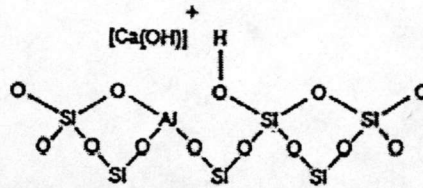
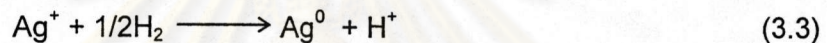
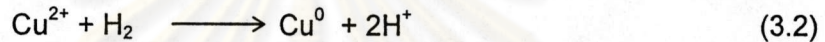


Figure 3.11 Water molecules co-ordinated to polyvalent cation are dissociated by heat treatment yielding Bronsted acidity [28].

was note to increase by hydrogen at 250-450 °C to increase with the rise of the reduction temperature[28].



The formation of Lewis acidity from Bronsted sites is depicted in Figure 3.12 [28]. The dehydration reaction decreases the number of protons and increases that of Lewis sites.

Bronsted (OH) and Lewis (-Al-) sites can be present simultaneously in the structure of zeolite at high temperature. Dehydroxylation is thought to occur in ZSM-5 zeolite above 500 °C and calcination at 800 to 900 °C produces irreversible dehydroxylation which causes defecion in crystal structure of zeolite.

Dealumination is believed to occur during dehydroxylation which may result from the steam generation within the sample. The dealumination is indicated by an increase in the surface concentration of aluminum on the crystal. The

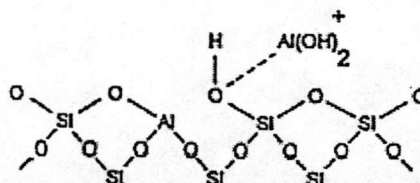


Figure 3.14 The enhancement of the acid strength of OH groups by their interaction with dislodged aluminum species [28].

The enhancement of the acid strength of OH groups is recently proposed to be pertinent to their interaction with those aluminum species sites tentatively expressed in Figure 3.14[28]. Partial dealumination might therefore yield a catalyst of higher activity while severe steaming reduces the catalytic activity.

3.3.3 Basic Sites

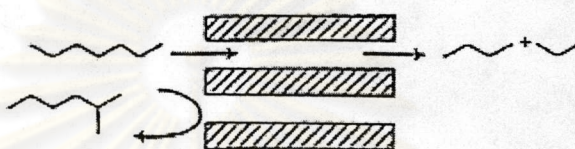
In certain instances reactions have been shown to be catalyzed at basic (cation) sites in zeolites without any influence from acid sites. The best characterized example of this is that of K-Y which splits n-hexane isomers at 500°C. The potassium cations has been shown to control the unimolecular cracking (β - scission). Feed radical mechanisms also contribute to surface catalytic reactions in these studies.

3.4 Shape-Selective Catalysis

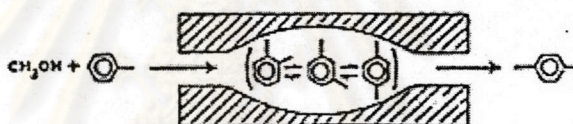
Many reactions involving carbonium ions intermediates are catalyzed by acidic zeolites. With respect to a chemical standpoint the reaction mechanisms are not fundamentally different with zeolites or with any other acidic oxides. What zeolite

add is shape selectivity effect. The shape selective characteristics of zeolites influence their catalytic phenomena by three modes; reactants shape selectivity, products shape selectivity and transition states shape selectivity [27,35,36]. These type of selectivity are predicted in Figure 3.15[27].

a) Reactants selectivity



b) Products selectivity



c) Transition states selectivity

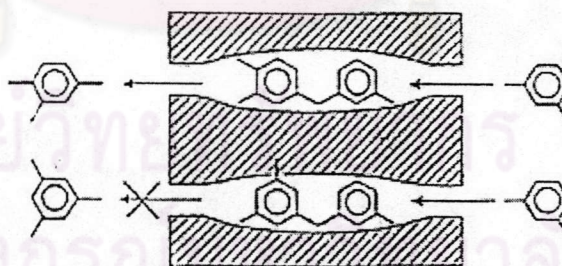


Figure 3.15 Diagram depicting the three type of selectivity[27].

Table 3.3 Kinetic diameters of various molecules based on the Lennard-Jones relationship [35].

	KINETIC DIAMETER (ANGSTROMS)
He	2.60
H ₂	2.89
O ₂	3.46
N ₂	3.43
NO	3.17
CO	3.76
CO ₂	3.30
H ₂ O	2.65
NH ₃	2.60
CH ₄	3.80
C ₂ H ₂	3.30
C ₂ H ₄	3.90
C ₃ H ₈	4.30
n-C ₄ H ₁₀	4.30
Cyclopropane	4.23
i-C ₄ H ₁₀	5.00
n-C ₅ H ₁₂	4.90
SF ₆	5.50
Neopentane	6.20
(C ₄ F ₉) ₃ N	10.20
Benzene	5.85
Cyclohexane	6.00
m-xylene	7.10
p-xylene	6.75
1,3,5 trimethylbenzene	8.50
1,3,5 triethylbenzene	9.20
1,3 diethylbenzene	7.40
1-methylnapthalene	7.90
(C ₄ H ₉) ₃ N	8.10



Reactant or charge selectivity results from the limited diffusibility of some of the reactants, which cannot effectively enter and diffuse inside crystal pore structures of the zeolites.

Product shape selectivity occurs as slowly diffusing product molecules cannot escape from the crystal and undergo secondary reactions. This reaction path is established by monitoring changes in product distribution as a function of varying contact time.

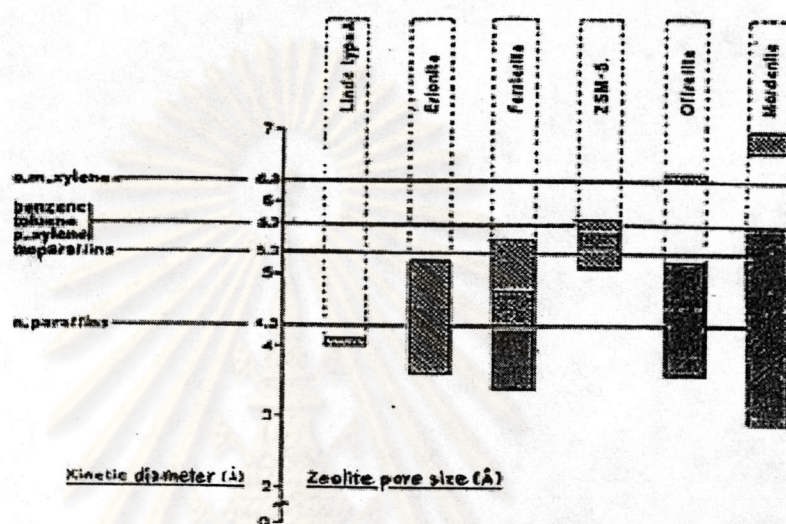



Figure 3.16 Correlation between pore size(s) of various zeolites and kinetic diameter of some molecules [35].

Restricted transition state shape selectivity is a kinetic effect arising from local environment around the active site, the rate constant for a certain reaction mechanism is reduced if the space required for formation of necessary transition state is restricted.

The critical diameter (as opposed to the length) of the molecules and the pore channel diameter of zeolites are important in predicting shape selective effects. However, molecules are deformable and can pass through openings which are smaller than their critical diameters. Hence, not only size

but also the dynamics and structure of the molecules must be taken into account.

Table 3.3 [37] presents values of selected critical molecular diameters and Table 3.4 [27] presents values of the effective pore size of various zeolites. Correlation between pore size(s) of zeolites and kinetic diameter of some molecules are depicted in Figure 3.16 [35].



ศูนย์วิทยทรัพยากร
จุฬาลงกรณ์มหาวิทยาลัย

Table 3.4 Shape of the pore mouth opening of known zeolite structures. The dimensions are based on two parameters, the T atom forming the channel opening (8, 10, 12 rings) and the crystallographic free diameters of the channels. The channels are parallel to the crystallographic axis shown in brackets (e.g. $\langle 100 \rangle$) [49].

STRUCTURE	4-MEMBER RING	10-MEMBER RING	12-MEMBER RING
Bikitaite	3.2x4.9[001]		
Brewsterite	2.3x5.0[100] 2.7x4.1[001]		
Cancrinite			6.2[001]
Chabazite	3.6x3.7[001]		
Dachiardite	3.6x4.8[001]	3.7x6.7[010]	
TMA-E	3.7x4.8[001]		
Edingtonite	3.5x3.9[110]		
Epistibite	3.7x4.4[001]	3.2x5.3[100]	
Erionite	3.6x5.2[001]		
Faujasite			7.4 $\langle 111 \rangle$
Ferrierite	3.4x4.8[010]	4.3x5.5[001]	
Gismondine	3.1x4.4[100] 2.8x4.9[010]		
Gmelinite	3.6x3.9[001]		7.0[001]
Heulandite	4.0x5.5[100] 4.1x4.7[001]	4.4x7.2[001]	
ZK-5	3.9 $\langle 100 \rangle$		
Laumontite		4.0x5.6[100]	
Levyne	3.3x5.3[001]		
Type A	4.1 $\langle 100 \rangle$		
Type L			7.1[001]
Mazzite			7.4[001]
ZSM-11		5.1x5.5[100]	
Merlinoite	3.1x3.5[100] 3.5x3.5[010] 3.4x5.1[001] 3.3x3.3[001]		
ZSM-5		5.4x5.6[010] 5.1x5.5[100]	
Mordenite	2.9x5.7[010]		6.7x7.0[001]
Natrolite	2.6x3.9 $\langle 101 \rangle$		
Offretite	3.6x5.2[001]		6.4[001]
Paulingite	3.9 $\langle 100 \rangle$		
Phillipsite	4.2x4.4[100] 2.8x4.8[010] 3.3[001]		
Rho	3.9x5.1 $\langle 100 \rangle$		
Stibite	2.7x5.7[101]	4.1x6.2[100]	
Thomsonite	2.6x3.9[101] 2.6x3.9[010]		
Yugawaralite	3.1x3.5[100] 3.2x3.3[001]		

3.5 Non - aluminosilicate Molecular Sieves

Advances in the area of new molecular sieve materials have come in the preparation of zeolite - like structure containing framework components other than aluminum and silicon exclusively. The aluminosilicate zeolites offer the ion exchange properties, higher thermal stability, high acidity and shape-selective structural features desired by those working in the areas of adsorption and catalysis. However, modification and subsequent improvement of these properties have served as a driving force for changing the composition of these microporous materials.

It is well accepted that gallium can easily be substituted for aluminum and germanium for silicon in aluminosilicate system, as these elements are in the same family of the periodic table. Gallosilicate, gallogerminate and germanium aluminate analogs of the known zeolites have been hydrothermally synthesized under conditions comparable to the zeolite molecular sieves. Other elements were found not to substitute so easily. In the crystallization of many zeolite structures, the relative amounts of silicon and aluminum in the reacting gel strongly influenced the crystallization of a particular structure. Attempts to substitute vastly different elements for either aluminum or silicon resulted in suppression of crystallization. It was the discovery of the strong structure - directing properties of the cation organic amine additives that fuelled new discoveries of different chemical compositions with zeolite - like structures. The graph in Figure 3.17 [27] show this explosion in new (non-zeolitic) molecular sieves patented relative to the reported new zeolite materials synthesized and the natural zeolite minerals known. The number of non - zeolite molecular

sieves reported is far greater than the number of microporous aluminosilicate zeolite materials as shown in the graph.

In addition to the gallosilicates, germanium aluminates, and gallogerminates synthesized prior to the use of organic additives, materials containing zeolite-type structures crystallized in the presence of organic cation have been claimed to contain boron, iron, chromium, cobalt, titanium, zirconium, zinc, beryllium, hafnium, manganese, magnesium, vanadium, and tin. Little characterization of the extent of incorporation has been presented for many of these materials. The most common structure claims to incorporate such elements is the ZSM-5 type framework.

However, it is well accepted that the ZSM-5 structure, strongly directed by the presence of the TPA cation, can easily crystallize in the pure silica form (silicate). Therefore, the possibility remain, without sufficient characterization to confirm incorporation, that this exclusively silica - containing structure could form metallosilicate reaction mixture, giving the characteristic X-ray diffraction pattern without incorporating the desired metal component into the structure. Boron, gallium, iron, and titanium have been sufficiently characterized to confirm structure incorporation.

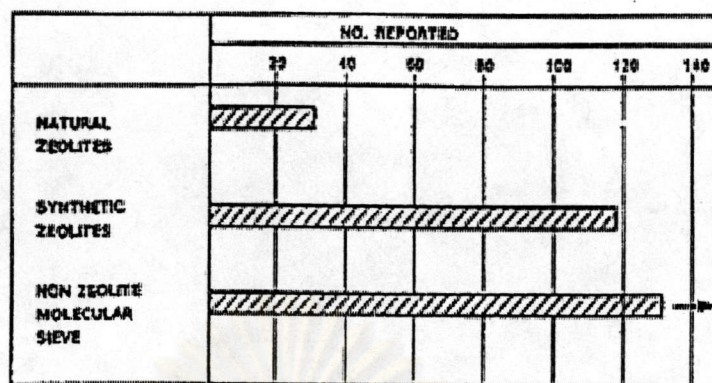


Figure 3.17 A comparison of the natural zeolites known and the number of zeolites synthesized within the last 30 years with the number of recently patented non-zeolite molecular sieves [27].

3.6 Acidity of Metallosilicate

The synthesis of zeolites containing various elements such as B, P, or Ge has been carried out for a long time. Since the discovery of ZSM-5 (aluminosilicate) and silicalite, many attempts have been made to synthesize the metallosilicate with the ZSM-5 structure. The isomorphous substitution of aluminum with other elements greatly modifies the acidic properties of the silicate. The elements introduced include, Be, B, Ti, Cr, Fe, Zn, Ga, and V. These elements were usually introduced by adding metal salts as one of the starting materials for the synthesis of the metallosilicate. It is also known that boron can be directly introduced by reacting ZSM-5 with boron trichloride. Metallosilicate with a ZSM-5 structure having metal M as a component will be denoted [M]-ZSM-5, hereafter. Silicate II (the framework topology of which is structurally identical to

is structurally identical to that of ZSM-11) can be transformed into gallosilicate with its reaction with NaGaO_2 in an aqueous solution.

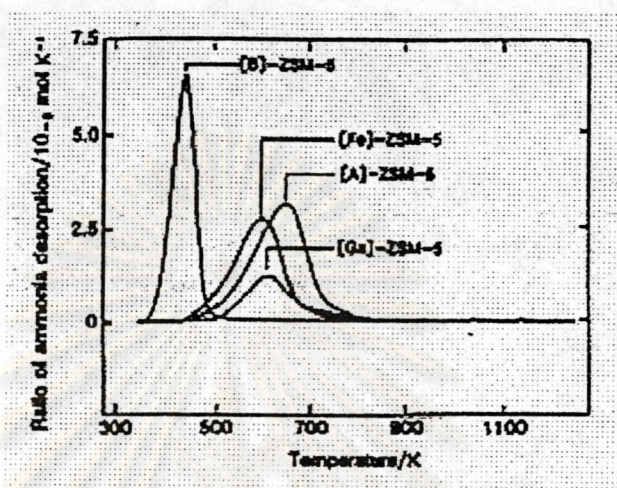
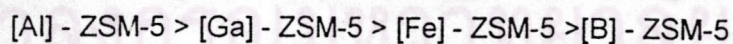


Figure 3.18 Temperature programmed desorption of ammonia from metallosilicate (Reported with permission by C. T - W. Chu, C. D. Chang, J. Phys. Chem., 89, 1571(1985)) [28].

Figure 3.18 [28] shows the TPD spectrum of ammonia adsorbed on various metallosilicate. The acid strength of metallosilicate changes in decreasing order as follows:



The band position of OH groups changes in conformity with TPD spectra. Thus, the OH band appears at 3610, 3620, 3630, and 3725 cm^{-1} for [Al]-, [Ga]-, [Fe]-, and [B]-ZSM-5, respectively. The fact that the acid

strength of [B]-ZSM-5 is much weaker than that of [Al]-ZSM-5 has been reported by several authors.

Table 3.5 Product distribution of the conversion of 1-butene over H-ZSM-5, H-[B]-ZSM-5 and Zn-[B]-ZSM-5[28].

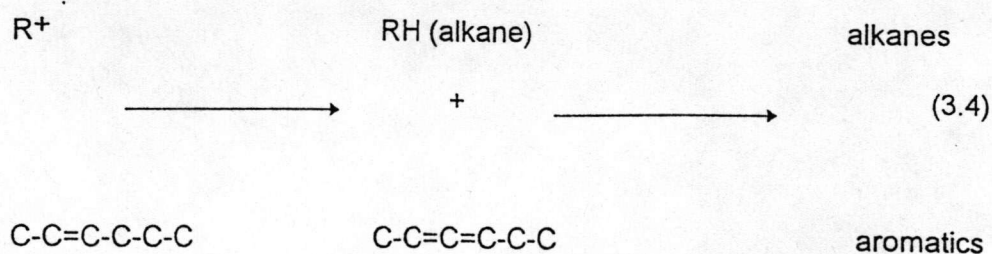
Catalyst	H-[Al]-ZSM-5	H-[B]-ZSM-5	Zn-[B]-ZSM-5
conversion/%	77.3	71.7	81.2
Products/% ¹¹			
C ₁ -C ₄ alkanes	41.3	5.1	6.3
C ₂ H ₄ +C ₃ H ₆	14.6	38.3	21.1
C ₄ H ₈ ¹²	6.2	28.3	27.7
C ₅ ⁺	2.4	25.3	7.0
aromatics	37.0	3.0	38.0

Reaction conditions, 773 K, W/F=5.3 g h mol⁻¹

1-butene=23.0 kPa

¹¹ carbon-number basis, ¹² including 1-butene

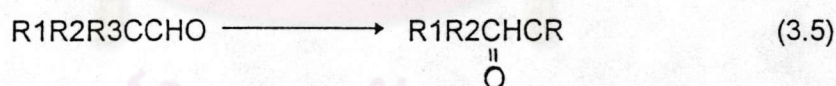
Weaker acid strength of [B]-ZSM-5 is confirmed also by catalytic reactions. Table 3.5 [28] shows the product distributions of 1-butene reaction over [B]-ZSM-5 and [Al]-ZSM-5 at 773 K. It is clear that there is a great difference in the product dismatic hydrocarbons, while over [B]-ZSM-5, lower alkenes are the main products. This indicates that the hydride transfer reactions from alkene to carbonium ion does not proceed over [B]-ZSM-5.



For the same reasons, alkenes are the main products in the conversion of methanol over [B]-ZSM-5, while [Al]-ZSM-5 is a unique catalyst for gasoline production.

The yield of aromatic hydrocarbons greatly increases by introducing zinc cations into [B]-ZSM-5 (Table 3.5). In this case, however, the yield of alkanes remains low. This is because the aromatics are formed by the direct dehydrogenation of olefins by the action of zinc species. As exemplified by this case, it is possible to achieve catalysis by metal cations at the same time suppressing catalysis by acid.

The acid strength of [Fe]-ZSM-5 can be inferred to be weak from the very low yield of alkanes and aromatics in the conversion of methanol to olefins. Holderich reported that ketone can be isomerized to aldehyde in a high selectivity over [B]-ZSM-5. ZSM-5 gave only low selectivity.



Since the acidic strength of [B]-ZSM-5 is weak, the role of the trace amount of aluminium impurity may not be negligible in their catalysts. Chu et al. examined the catalytic activities of [B]-ZSM-5 containing varying amounts of framework B for a number of acid-catalyzed reactions and concluded that the catalytic activity was due, if not entirely, to trace amounts (80-580 ppm) of framework aluminium [28].



3.7 Aromatic Hydrocarbons

Aromatic chemicals represent about 30% of the total of some 8 million known organic compounds[29]; the percentage of aromatic chemicals produced by the entire organic chemical industry is of the same order.

The importance of aromatics in hydrocarbon technology is, however, greater than the percentage figures indicate. Quantitatively, the most important processes in hydrocarbon technology are catalytic reforming to product gasoline, which has a worldwide capacity of around 350 Mtpa, and the carbonization of hard coal to produce metallurgical coke, on roughly the same scale. A characteristic of both processes is the formation of aromatics. The third most important process in hydrocarbon technology in terms of quantity is catalytic cracking, which is also accompanied by an aromatization, as is the important petrochemical process, steam cracking of hydrocarbon fractions.

The recovery and further refining of aromatics was the basis of the industrial organic chemistry in the middle of the last century. In the early 1920's, aromatic chemistry was complemented by the chemistry of aliphatics and olefins, which today, in terms of quantity, has surpassed the industrial chemistry of aromatics. From the beginning of industrial aromatic chemistry there have been fundamental new developments in the production of aromatics. Until the 1920's, coal tar and coke-oven benzole were virtually the sole sources of aromatics available on an industrial scale. Coal tar contains a host of widely used aromatic compounds, such as benzene, toluene,

naphthalene, anthracene and pyrene, as well as styrene and indene. In addition coal tar contains some important recoverable aromatic compounds with hetero-atoms, such as phenols, anilines, pyridines and quinoline.

As the growing demand for some coal-tar constituents for the development of mass-produced plastics, such as phenolic resins and polystyrene, and the increasing production of explosives could not be met by coal tar alone, new sources of aromatics were developed, starting from petroleum. The development of the production of reformat-gasoline and steam cracking of petroleum fractions has made two further feedstock sources for the production of aromatics available today; renewable raw materials are also used for the manufacture of aromatics, albeit on a much smaller scale.

Processes for the refining of crude aromatics, in common with methods for their further processing, are complicated by the occurrence of by-products; individual aromatics are usually accompanied by associated products, and must be isolated by subsequent separation processes. Aromatic chemistry is characterized by the high reactivity of the π -electron system, which enables substitutions to take place not only at one position in the aromatic ring, but also, especially for polynuclear aromatics, at several different sites, thus leading to isomers as well as multiple substitution. Refining processes have, therefore, to be optimized to produce the desired compounds in pure form from the crude products. Thus, industrial aromatic chemistry involves close collaboration between chemists and process engineers.

The present applications and future developments of aromatic chemicals are characterized by a number of inherent properties. These are in particular:

1. the facile substitution and high reactivity, which can be further increased by the introduction of suitable substituents,
2. the relatively easily activated π -electron system which, coupled with auxochromic groups, is capable of absorbing part of the spectrum of light and is used in the production of dyes and pigments,
3. the high solvent power, especially of alkylated derivatives,
4. the high C/H ratio, which renders polycyclic aromatics particularly suited to the production of high-value industrial carbon products, such as premium coke, graphite and carbon black, and
5. the affinity and tendency for association, which make aromatic molecules suitable mesogens for the formation of liquid-crystal line phases.

Approximately 800,000 tpa of organic dyestuffs (dyes, pigments and optical brighteners) are produced worldwide. Since the beginning of the industrial production of organic dyestuffs, aromatics have been the dominant raw materials for this group of product.

3.7.1 Aromatic Character. The Huckel $4n + 2$ rule

We have defined aromatics compounds as those that resemble benzene. But just which properties of benzene must a compound possess before we speak of it as being aromatic? Besides the compounds that

contain benzene rings there many other substances that are called aromatic; yet some of these superficially bear little resemblance to benzene.

What properties do all aromatic compounds have in common?

From the experimental standpoint, aromatic compounds are compounds whose molecular formulas would lead us to expect a high degree of unsaturation, and yet which are resistant to the addition reactions generally characteristic of unsaturated compounds. Instead of addition reactions, we often find that these aromatic compounds undergo electrophilic substitution reactions like those of benzene. Along with this resistance toward addition-and presumably the cause of it - we find evidence of unusual stability: low heats of hydrogenation and low heats of combustion. Aromatic compounds are cyclic-generally containing five-, six-, or seven-membered rings - and when examined by physical methods, they are found to have flat (or nearly flat) molecules. Their protons show the same sort of *chemical shift* in NMR spectra as the protons of benzene and its derivatives.

From a theoretical standpoint, to be aromatic a compound must have a molecule that contain *cyclic clouds of delocalized π electrons above and below the plane of the molecule*; furthermore, *the π clouds must contain a total of $(4n+2)$ π electrons*. That is to say, for the particular degree of stability that characterizes an aromatic compound, delocalization alone is not enough. There must be a particular number of π electrons: 2 or 6 or 10, etc. This requirement, called the $4n+2$ *rule* or Huckel rule (after Erich Huckel, of the Institut fur

Theoretische Physik, Stuttgart), is based on quantum mechanics, and has to do with the filling up of the various orbitals that make up the π cloud. The Huckel rule is strongly supported by the facts.

3.7.2 Production of Aromatic Hydrocarbons with Zeolites

3.7.2.1 Aromatics from alcohols

Methanol is principal feedstock for the production of aromatic gasoline with zeolite catalysts

The first part of a plant, which uses the MTG process and has a planned final capacity of 800,000 tpa of gasoline with an octane rating of 92 to 94, is already in operation in New Zealand; the methanol is produced from natural gas.

Until 1986, UK - Wesseling, in collaboration with Mobil Oil and Uhde operated a pilot plant with a capacity of 25 t/d in West Germany, to optimize the fluidized - bed process.

Against the background to reduce the dependence of motor fuel on crude oil, *Mobil Oil* developed the Methanol to Gasoline (MTG) process to convert methanol to gasoline. Since methanol can be produced not only from crude oil but also from natural gas and coal by currently available technology, the MTG process is not dependent on crude oil as a raw material.

Figure 3.19 shows the flow diagram for the two stage Mobil Oil fixed - bed process.

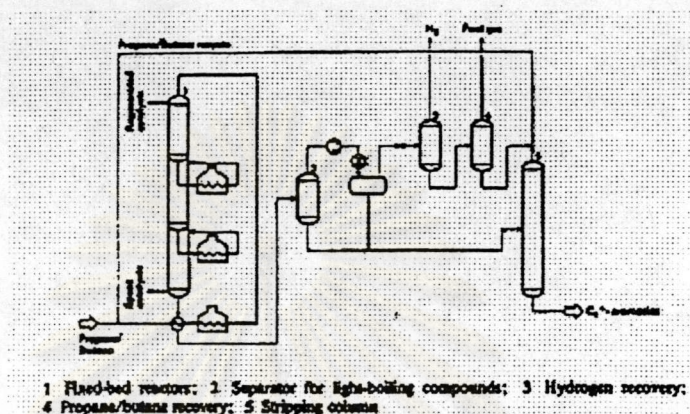


Figure 3.19 Flow diagram for the Mobil Oil fixed - bed process [29]

The reaction is carried out at a pressure of 20 bar and a temperature of 380 °C. The process produces 44% of hydrocarbons along with 56% of water. In terms of its composition and characteristics, such as octane rating boiling range and other specifications, the gasoline corresponds to currently - used motor gasolines.

Pentasil zeolites are used as catalysts, since their shape-selectivity leads to the formation of hydrocarbons with a carbon number below 11; in terms of boiling point, this corresponds to conventional gasoline.

3.7.2.2 Aromatics from short-chain alkanes [38]

Naphtha feedstock currently represent about 80% of the production cost of BTX. It is therefore attractive to substitute a less expensive material for

naphtha. This is the case for liquefied petroleum gas (LPG) mainly composed of propane and butane, which is overproduced and costly to transport. There exist three main processes for conversion of LPG into BTX

1. The M₂-forming process

With the M₂-forming process, proposed by Mobil, a large variety of feedstocks such as pyrolysis gasoline, unsaturated gases from catalytic cracking, paraffinic naphtha and LPG can be converted into aromatics. Depending on the reactivity of the feedstock, the operating temperature varies significantly, ranging from below 370 °C for alkenes to 538 °C for propane. H-ZSM-5 was chosen as a catalyst. Although remarkably stable in comparison with conventional acidic catalysts, H-ZSM-5 deactivates by coke deposition and the aromatic production requires a cyclic process. This purely acid catalyst (hence M₂-forming) seems to be interesting only for the production of high octane compounds from pyrolysis gasoline or paraffinic naphthas. Indeed, bifunctional catalysts are necessary to convert LPG into aromatics and hydrogen. Using pure butane as a feed leads to 65.9 wt.-% of aromatics, 5.2% of hydrogen and 28.9% of fuel gas. The aromatic cut contains about 92 wt.-% BTX.

The Grangemouth unit has a 1000 bbl/d capacity. The following yields were obtained from the conversion of LPGs: Aromatics 65 wt.-% (benzene 9.5 wt.-%; toluene 27.3 %; xylenes 13 %, others 5.2 %); hydrogen 6 %; fuel gas 29 %. The catalyst life is expected to be about two years. In addition a slightly modified catalyst has been announced. The demonstration unit closed down at the end of 1991.

When propane is used as a feedstock, the aromatic yield announced is 63.1 wt.-% and the hydrogen yield is 5.9 wt.-%. Fuel gas (31 wt.-%) is also produced.

3. The Aroforming process

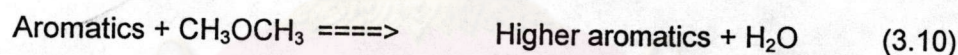
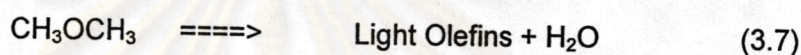
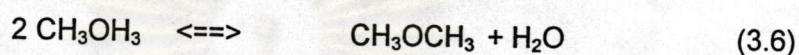
It is also of interest to convert light naphtha feedstocks (especially C₅ and C₆ alkanes) into aromatics for petrochemical purposes. The Cyclar process is not supposed to convert these rich C₆ cuts while the aroforming process, developed by IFP and SALUTEC, has been designed to aromatize a large range of aliphatic hydrocarbons, either LPGs or light naphthas. The catalyst is a shape selective zeolite doped with metal oxides.

The process is based on multiple fixed bed isothermal tubular reactors, some of which run reaction mode, while the others are under regeneration. The aroforming technology is convenient not only for large capacity units but also for low ones.

The following yields are found when a light naphtha is converted through the aroforming process; Aromatics 54.9 wt.-% (benzene 12.2 %, toluene 21.9 %, C₈ aromatics 12.5 %, others 8.3 %); hydrogen 2.9 %, C₁-C₂ : 27.4 %; C₃ 14.8 %. For LPG conversion, the results are close to those obtained with the Cyclar process.

3.8 Reaction Mechanism of Methanol to Aromatics

The reaction of methanol to hydrocarbon products is vigorously exothermic, with a theoretical adiabatic temperature rise of about 600 °C. The reaction path is believed to pass through a number of series and parallel steps. The mechanism is complex and is discussed elsewhere. A simplified path is given below[31,39].

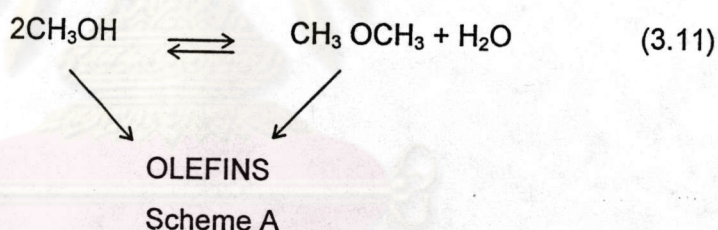


The first step in the reaction sequence is the dehydration of methanol to an equilibrium mixture of dimethylether (DME), methanol and water. The DME then reacts further to form a mixture of light olefins. As the concentration of DME is depleted, the equilibrium of reaction 3.4 is disturbed and further dehydration of methanol takes place. The DME alkylates the light olefins (mostly propylene and butenes) to higher olefins, which can then further react with one another to form aromatics and paraffins. If any residual DME remains at the point where aromatics form, those aromatics are readily alkylated to higher carbon number of C₁₀. The heaviest component is durene (1,2,4,5-tetramethylbenzene), which lies near the high

end of the gasoline boiling range. No components with normal boiling points above the gasoline boiling range are produced[36].

The early work of Chang [30] showed that, high temperature favours selectivity to light olefins. Mobil found that by combining the factors of reduced catalyst activity with high operating temperatures, it was possible to switch the Methanol to Gasoline (MTG) selectivity towards an olefin rich spectrum. This route was named the Methanol To Olefins (MTO) process, and gives a product that is rich in propylene and butenes together with a good aromatic rich C₅+gasoline fraction.

Voltz and Wise [37] has proposed scheme A to contain a direct path to olefins from methanol:



The reaction path formation may be viewed essentially as composed of three key steps - ether formation, initial C-C bond formation, and aromatization with H-transfer. The final stages, comprising olefins condensation, cyclization and H-transfer over acidic catalysts, have been well studied and proceed via classical carbenium mechanisms [40-42].

The mechanism of polymethylbenzenes formation will, however, be discussed since these compounds are peculiar to the methanol transformation reaction.

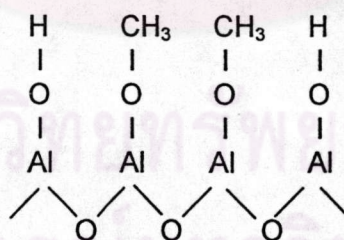


3.8.1. Ether formation

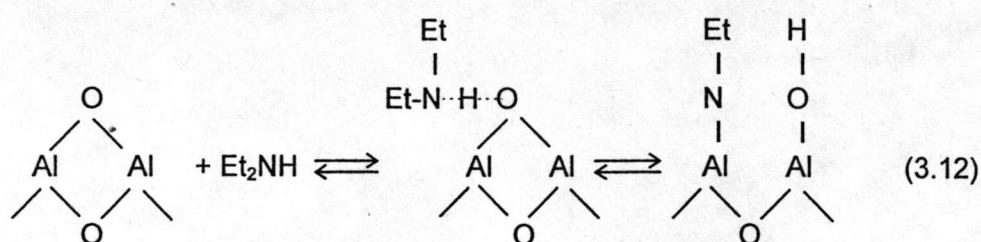
The mechanism of ether formation from alcohols over oxide catalysts, particularly Al_2O_3 , has been extensively investigated. The bulk of work has concentrated on alcohols having β -hydrogens. Several comprehensive surveys have been published [43-46].

In contrast, the literature on methanol dehydration is relatively sparse. Methanol etherification is similar in many respects to that of the higher alcohols; however, since methanol lacks a parent olefin, sufficient differences may be found as to warrant its discussion here.

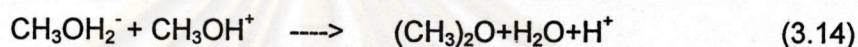
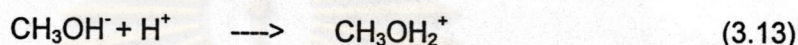
The dehydration of methanol on alumina and amorphous silica-alumina monitors the effect of a series of nitrogenous poisons (various amines and N-heterocycles) or dimethylether formation. Silica-alumina is irreversibly poisoned, while alumina is reversibly poisoned. This is taken as evidence that their action over alumina involved surface methoxy groups:



This interpretation is based on the assumption that bases such as diethylamine dissociatively but reversibly chemisorb on alumina.



Because of the greater nucleophilicity of N vs O, the nitrogenous base competes with methanol for the surface oxygen, thereby inhibiting methoxylation. On the otherhand, the reaction over silica-alumina involves Bronsted sites, which are strongly poisoned by nitrogen base, forming stable quaternary ions. According to these investigators ether formation over silica-alumina may be represented by the following scheme:



The kinetics of methanol dehydration over silica-alumina at 160-200° C and the rate expression can derive as follow:

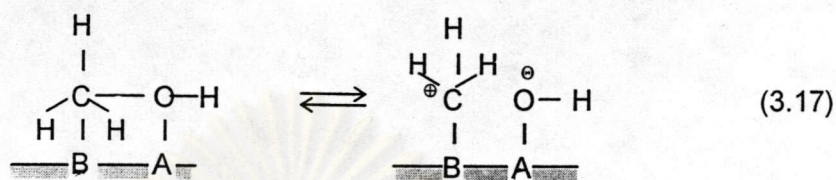
$$V = k_a \sqrt{P_a} / (1 + \sqrt{P_a}) \quad (3.15)$$

where P_a is the alcohol partial pressure. It was concluded that the rate-limiting step cannot be the interaction of two surface alcoholate groups, which would lead to a rate equation of the form

$$r = k\theta^2 = k_a P / (1 + aP)^2 \quad (3.16)$$

At low pressures the reaction order would be unity, which is not in agreement with the observed half-order. Figueras et al. proposed two modes of chemisorption, both of which assumed the concerted action of acidic and basic centers. Nucleophilic attack on carbon by the basic site would generate CH_3^+ , which then interacts with an acid-generated surface methoxy group to give ether. The observed half-order was rationalized on the ground that one of the species, CH_3O or

CH_3 must be reversibly adsorbed. Primary carbonium ions are much less stable than alkoxide structures, and therefore equilibrium with the undissociated species would be readily established:

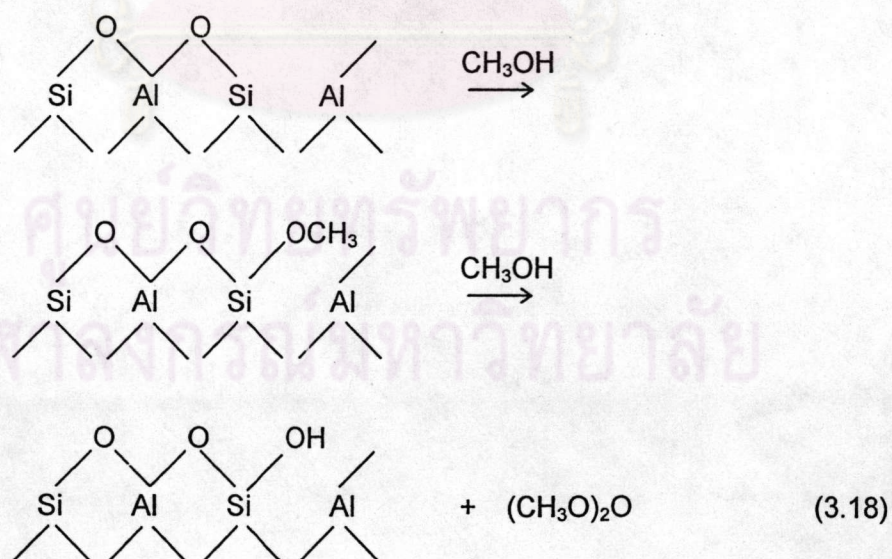


The thermal decomposition of methanol adsorbed on alumina was investigated by using deuterium labeling. Desorption of methanol started at 77°C . At $T > 77^{\circ}\text{C}$, significant concentrations of CH_2O , H_2O , and CH_3OCH_3 were observed, and above 427°C , CO was predominant while CH_4 was significant. Co-adsorption of CD_3OD and CH_3OH was carried out. Under desorption at $T < 237^{\circ}\text{C}$, the ether contained on CH_3OCH_3 , CH_3OCD_3 and CD_3OCD_3 , while at higher temperatures deuterium distribution became random. Thermal decomposition of $\text{CH}_3\text{OH}_{\text{ad}}$ in the presence of gaseous CD_3OCD_3 gave only CH_3OCH_3 , indication that ether is formed by a bimolecular reaction between adjacent surface methoxides.

Schmitz [46] studied the dehydration of methanol over silica-alumina at 289 – 418°C and found that the reaction becomes first-order in methanol at the higher temperatures. Interestingly, Schmitz observed an induction period, possibly the result of the initial formation of surface carboxylate groups, which, though not ether intermediates, could nevertheless influence the initial rate of dehydration by occupying active sites. Another explanation might involve competitive sorption of product water prior to establishment of steady-state with respect to surface hydroxyl concentration.

Detrekoy and Kallo [47] investigated the dehydration of methanol over clinoptilolite at various temperatures. At 25° C the 3620 cm⁻¹ band (acidic OH on clinoptilolite) disappears and two bands at 2950 and 2840 cm⁻¹ (CH stretching) appear. Upon evacuation, the CH bands decreased significantly; however, the OH band did not reappear. This indicated that only weakly adsorbed methanol is removed. Absorption at 160°C followed by evacuation caused only a partial disappearance of the 3620 cm⁻¹ band and a lower intensity of the 2950 and 2840 cm⁻¹ bands. At 400° C, methanol can be completely removed and the CH bands are shifted to 2860 and 2960 cm⁻¹, indicating the presence of surface methoxyls.

Detrekoy and Kallo found that methanol dehydration also occurs on dehydroxylated (at T > 400° C) clinoptilolite. They attribute this to the formation of Bronsted sites from Lewis sites by hydration during reaction with methanol. The following mechanism was proposed:



Further reaction would be catalyzed by the acidic OH groups thus generated.

In a study of methanol reaction on synthetic germanic near-faujasite using ^{13}C -NMR, Derouane et.al. [48] observed partial methoxylation of the surface at 300°C , with ether formation. Surface methoxyls could be hydrolyzed with water back to methanol at 25°C . Additional small amounts of dimethyl ether and surface formate were also found after hydrolysis.

In summary, the weight of evidence favors the intermediacy of surface alkoxyls in ether formation from alcohols. Beranek and Kraus [49] conclude that the mechanism involves essentially a nucleophilic substitution whereby the surface alkoxide is attacked by another molecule, either from the gas phase or from a weakly adsorbed state. Arguments in support of this mechanism were summarized as follows:

1. "Similar products are obtained by the decomposition of metal alkoxides containing non-hydrogens and by the reaction of corresponding alcohols on alumina at lower temperatures".
2. "Acetic acid and pyridine are poisons for the formation of ethers".
3. "The different degrees of water inhibition on the ether and olefin formation from ethanol on alumina, and the agreement of ether/ethylene selectivity ratios found experimentally with those calculated by the Monte Carlo simulation of the hydrated surface of alumina".
4. "Correlation between the rate of ether formation from methanol and the surface concentration of ethoxide species determined by IR spectroscopy".
5. "The positive value of the Taft reaction parameter for the formation of ether in contrast to negative values for the olefin formation on the same catalyst".

The second part of Statement 5 applies only to C_2^+ alcohols.

3.8.2 Hydrocarbon Formation

The mechanism of initial C-C bond formation from methanol is an unresolved question at present. Hypothetical mechanisms abound in the literature, and run the gamut from carbene to free radical schemes. As of this writing, however, little supporting experimental evidence has appeared. It seems appropriate, nevertheless, to survey and discuss the diverse entries in the "mechanism sweepstakes".

3.8.2.1 Via Surface Alkoxy

Among contemporary investigators, the first to consider this question were Topchieva and collaborators in connection with a study of the adsorption of methanol vapor on SiO_2 , $SiO_2-Al_2O_3$ and Al_2O_3 surfaces. It was found that a portion of the methanol was irreversibly adsorbed on $SiO_2-Al_2O_3$ and Al_2O_3 , which upon heating and pumping to $400^\circ C$ evolves C_2H_4 , C_2H_6 , CO , and CO_2 . The formation of surface methoxy groups was regarded as the primary step. Hydrocarbon formation was considered to occur by condensation of methoxy groups, accompanied by dehydration and H-transfer. The mechanistic details of this condensation were not specified. Subsequently, Heiba and Landis [50] showed that the thermolysis products of aluminum alkoxides are virtually identical to the products of alumina-catalyzed decomposition of alcohols or ethers, as shown in Table 3.2. It is seen that the main products are CH_4 , H_2 , CO , $(CH_3)_2O$, and smaller amounts of C_2H_4 and C_3H_6 . Based on the observation that $Al(OCH_2\Phi)_3$ decomposed more readily than $Al(OCH_3)_3$, it was concluded that cleavage of the C-O bond is a heterolytic process, with the flow of

electrons in the direction of Al, leaving a positively charged carbon moiety as the reactive intermediate. A negative activation entropy was observed, suggesting a cyclic transition state. A free radical mechanism was rejected on the basis of negligible reactivity over nonacidic solids, e.g., quartz, at temperatures up to 450°C.

Table 3.6 Decomposition of Methyl Derivatives [50].

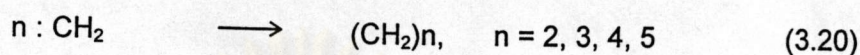
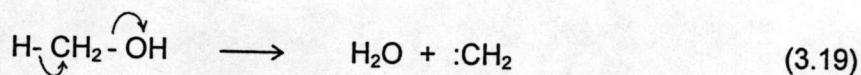
Product	Al(OCH ₃) ₃ at 385°C(mol%)	CH ₃ OH over Al ₂ O ₃ at 450°C 0.5 LHSV	(CH ₃) ₂ O over Al ₂ O ₃ at 450°C 0.5 LHSV
CH ₄	22.5	Major	Major
H ₂	35.2	Major	Major
CO	31.1	Major	Major
C ₂ H ₄	1.3	Minor	Minor
C ₃ H ₆	2.5	Minor	Minor
(CH ₂)O	7.1	Minor	Major
Other	0.3	Minor	Major

In a later study the thermal decomposition of methoxides of Na, Mg, and Al and the compound Na[Al(OMe)₄] was reported by Pfeifer and Flora [51]. Ethene was the only hydrocarbon product observed.

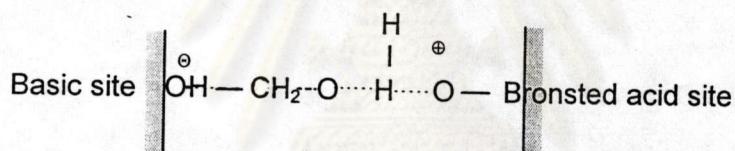
3.8.2.2 Carbenes and Carbenoids

Venuto and Landis proposed an α -elimination mechanism to account for olefins formed during methanol dehydration to dimethyl ether over NaX at 260°C, as reported by Mattox [52], and from methanol reaction over ReX and ZnX at 330-390°C, as Observed by Schwartz and Ciric [53]. According to this view, methanol

adsorbed on the zeolite surface loses water to form a divalent carbenoid species, which then polymerize to form olefins:

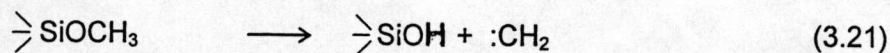


Swabb and Gates studied the dehydration of methanol over H-mordenite at 155-240° C. Traces of olefin were detected at 240° C. It was speculated that the olefins were formed by an α -elimination mechanism, where bond scission is facilitated by cooperative action of acidic and basic sites in the zeolite lattice:



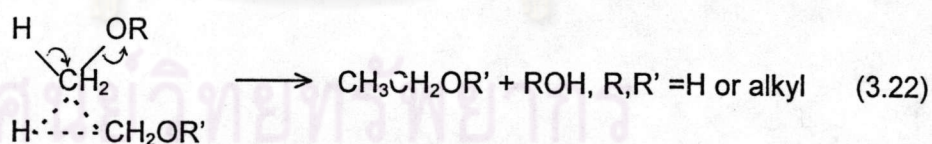
Salvador and Kladning [54] investigated the surface reactions of methanol on HY and NaY at 20-371° C using IR, GLC, adsorption isotherm, and TGA techniques. At room temperature, physical adsorption occurs on both zeolites. With HY, methoxylation of surface hydroxyl groups begins at 20° C, reaching a maximum at 130° C. At 120° C, dimethyl ether formation begins and reaches a maximum at 210° C, and around 250° C secondary cracking reactions occur forming predominantly butane and propene. This was accompanied by darkening of the catalyst due to coking which was enhanced with a further temperature increase. Salvador and Kladnig favored an α -elimination mechanism to explain olefin formation. They differed with the acid-base mechanism of Swabb and Gates,

proposing that the generation of carbenoid species occurs by decomposition of the methoxylated surface:

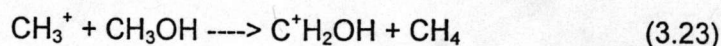


Condensation of the carbene would give olefin. Alkanes were assumed to arise via H-transfer reactions.

An α -elimination mechanism involving a carbenoid intermediate was also proposed by Chang and Silvestri for methanol reaction over ZSM-5. However, it was considered unlikely the olefins were formed by polymerization of the diradical intermediate. On view of the high reactivity of carbenes, the probability of such an event would be low, as demonstrated in studies on ketene photolysis. By the same token, the presence of free carbenes would be unlikely. Rather, a concerted reaction between methylene donor and acceptor was proposed involving simultaneous α -elimination and sp^3 insertion into methanol or dimethyl ether as the primary step.



An ionic mechanism involving methyl cations was rejected since these species would be expected to form methane readily via hydride abstraction from methanol, dimethyl ether, or hydrocarbons. The reaction



is extremely rapid in the gas phase. However, methane normally accounts for $\leq 1\%$ of the hydrocarbons formed over ZSM-5. Note also that $\text{C}^+\text{H}_2\text{OH}$ could deprotonate to formaldehyde which is not observed over ZSM-5.

The presence of small amounts of methyl ethyl in the products of methanol conversion over ZSM-5 was reported by Chang and Silvestri. Cormerais et al. found MeOEt among the products of dimethyl ether decomposition over silica-alumina at 423 K. This compound could either be a key reaction intermediate or simply a secondary product of the methanol-to-ethene reaction. From kinetic evidence, Cormerais et al. deduced that this compound was not formed via reaction of Me_2O with ethene. It was determined that in the presence of excess ethene, amounting to 30X that of the products from Me_2O , the rate of MeOEt formation from Me_2O was increased by only a factor of 5. More significantly, the formation of propene from MeOEt was more than 10 times faster than from Me_2O . In view of the observed unreactivity of ethene, it was concluded that propene is formed by two successive CH_2 insertions into Me_2O , leading to MeOPr, which cleaves to propene. Another set of experiments gave analogous results for C_4 hydrocarbons.

ศูนย์วิจัยทรัพยากร
จุฬาลงกรณ์มหาวิทยาลัย

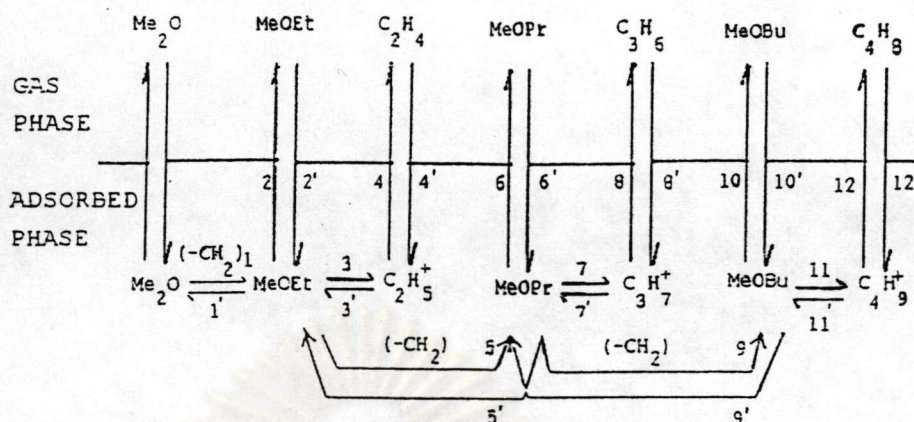
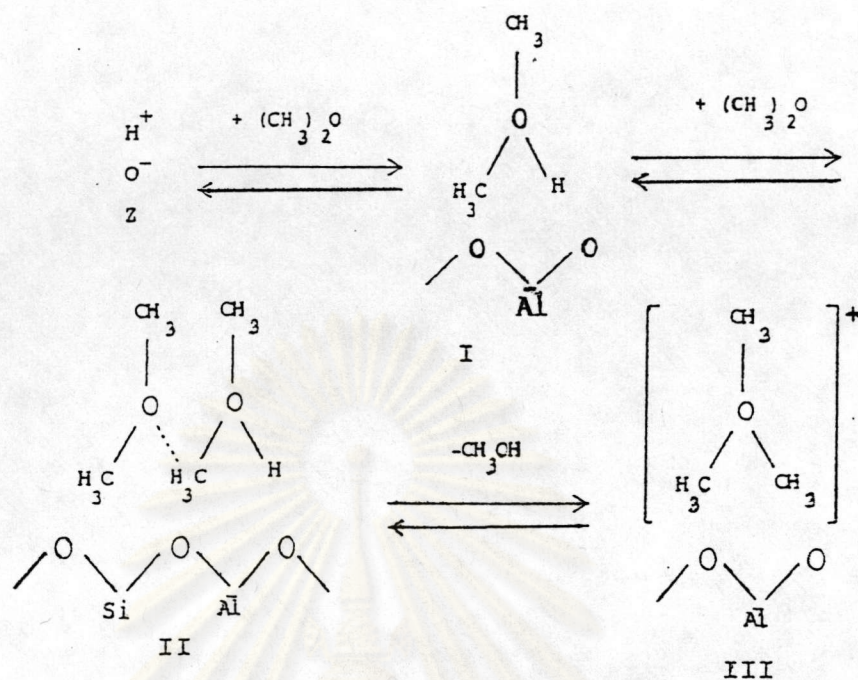


Figure 3.21 "Rake" mechanism for dimethyl ether conversion to hydrocarbons [55].

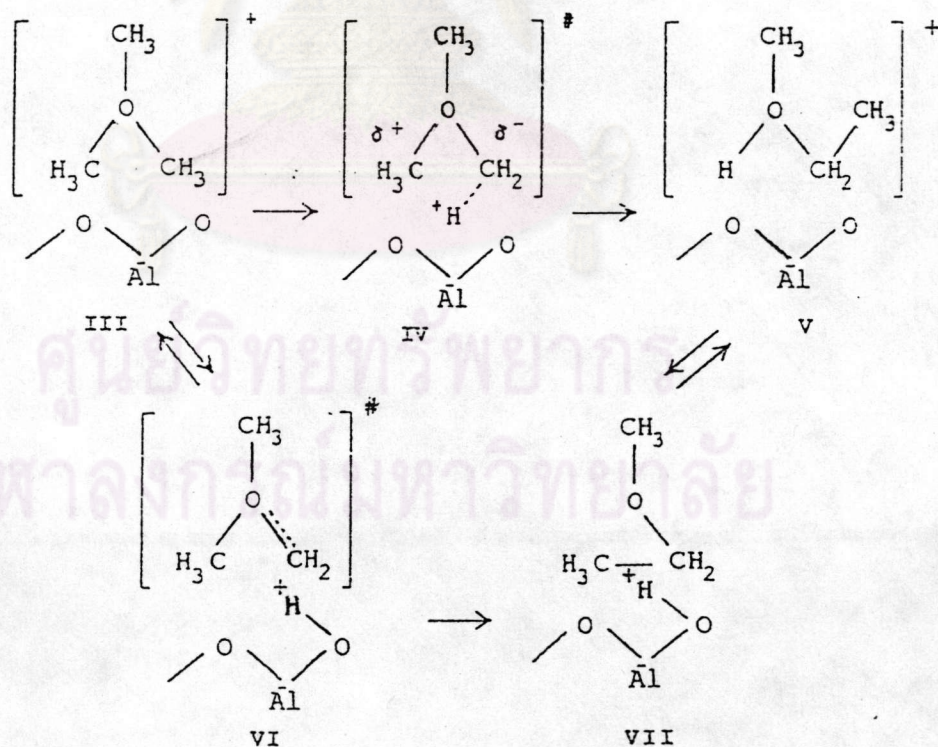
Cormerais et al. [55,56] proposed a chain growth "rake mechanism," Figure 3.8, to explain their results. In this scheme, chain growth occurs by carbene insertion into surface alkoxy species, which are transformed into olefins via carbenium ions.

3.8.2.3 Oxonium Ions and Yields

In their mechanism Chang and Silvestri left open the question of stabilization of the intermediate carbene in the transition state. A plausible resolution of the question may be found in the mechanism of van den Berg et al. [57]. In their view, dimethyl ether from methanol dehydration reacts with a Bronsted acid site to form a dimethyloxonium ion I, which reacts with another molecule of dimethyl ether to form, via II, and after elimination of methanol, a trimethyloxonium ion III:



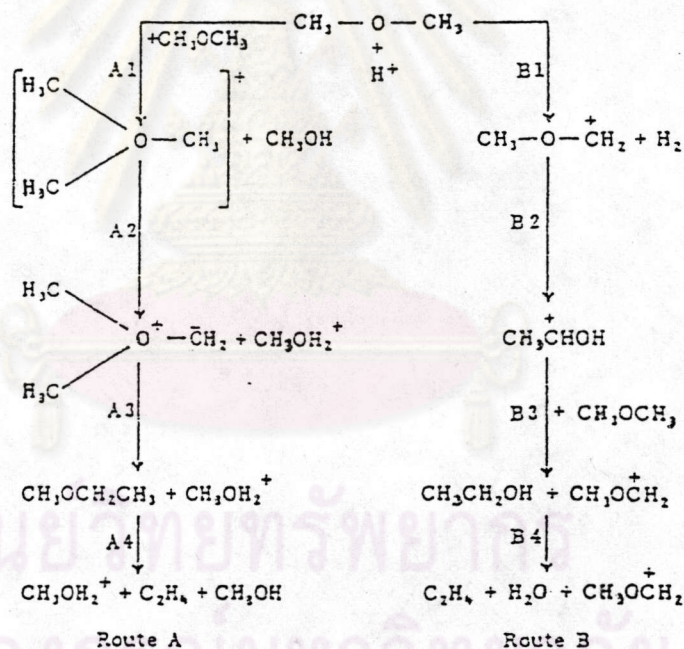
the critical step in their proposal is a Stevens-type intramolecular rearrangement of the trimethyloxonium ion III to a methylethyloxonium ion V :



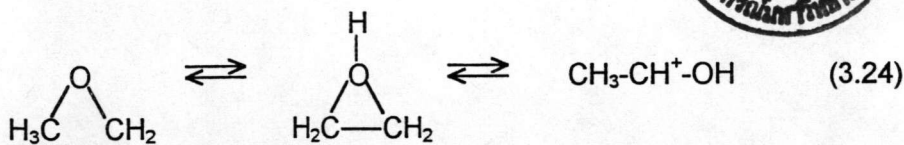
Structure VI , which is equivalent to the oxonium ylid $(\text{CH}_3)_2\text{O}^+\text{CH}_2$, is seen to contain the stabilized C_1 carbenoid species. Cis-insertion of the carbenoid into the adjacent

C-O leads to C-C bond formation. The formation of ylid depends on the assumption that the conjugate basic sites in ZSM-5 are sufficiently strong to induce polarization of a C-H bond on a methyl group. As indicated previously, the ab initio field calculations of Bern and Juries [58] lend support to this assumption.

An alternate cationic mechanism involving carboxoniumions was considered by van den Berg [59]. In this variation the scaboxoniumion is generated by hydride abstraction. Van den Berg presented the following scheme comparing the steps in the alkoxonium Route (A) and the carboxonium Route(B).



A major difference is found between Steps A2 and B2. However, ab initio calculations indicate that although the 1-hydroxyethyl cation is more stable than the methoxymethyl cation, the energy barrier separating the two is on the order of 260 kJ/mole, assuming that the rearrangement proceeds through the O-protonated oxirane:



this is comparable to the expected energy barrier of Step A2. Step A3 is highly exothermic and, in view of the behavior of the N-analogue, is expected to have a low activation energy. Figure 3.4 is an energy diagram comparing Routes A and B. It was concluded that Route A, involving the trimethyloxonium ion, is favored.

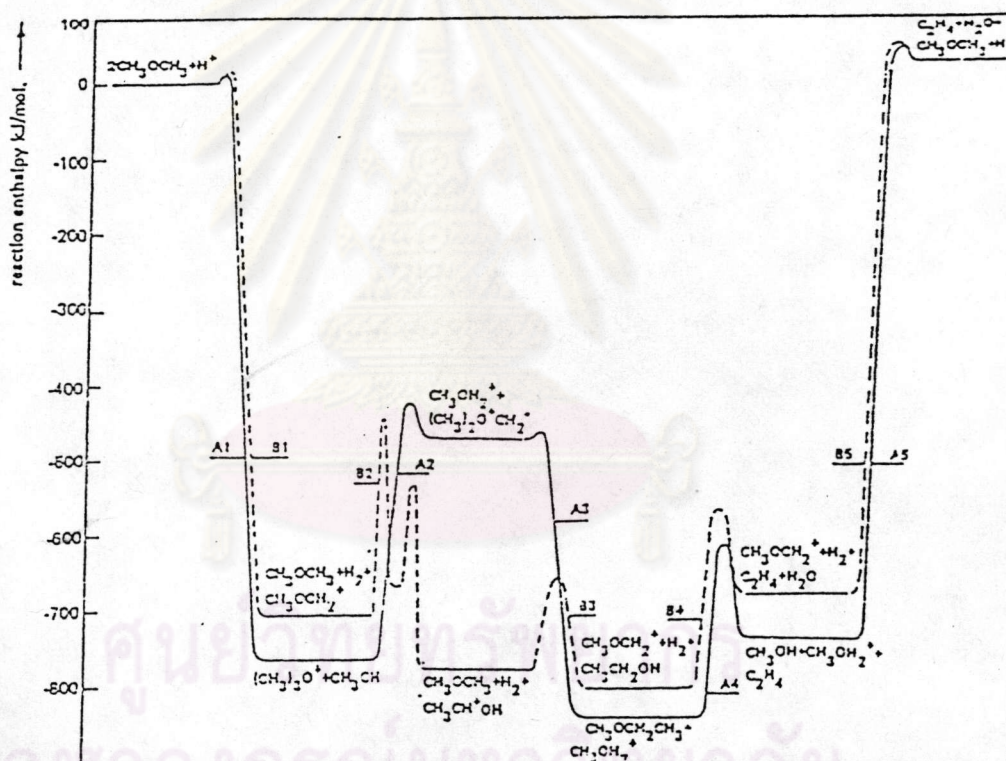


Figure 3.22 Energy diagram for Routes A and B [59].

According to van der Berg, kinetics of dimethyl ether reaction over HZSM-5 is zero-order at 227-300° C. Chang and Lang found the reaction order of

methanol decomposition over HZSM-5 at 350° C to be zero-order up to about 60% conversion, and increasing in order at higher conversions, suggestive of Langmuir-Hinshelwood behavior. This is consistent with van den Berg's proposal that the formation of adsorbed alkoxyoxonium species is favored, with the C-C bond of formation as the most demanding step. However, van den Berg observed an anomalous temperature effect, illustrated in the Arrhenius plot of Figure 3.10. To explain this phenomenon it was proposed that at 227-260° C, C-C bond formation proceeds via the intramolecular rearrangement of trimethyloxonium ions while at higher temperatures a concerted reaction between dimethyl ether and alkyl cations, with the oxoniumion as the transition state, becomes significant.

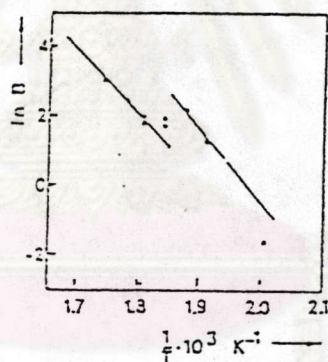
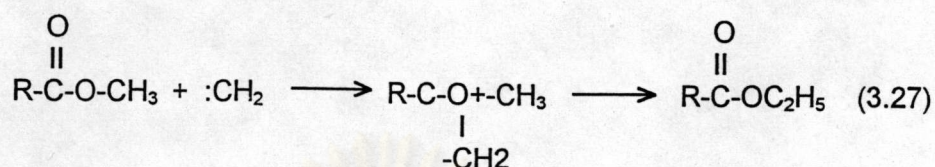


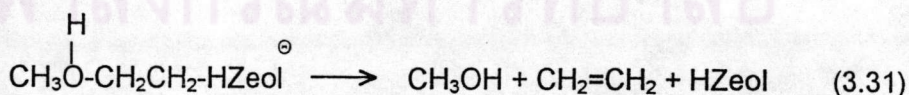
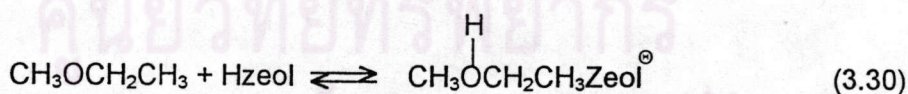
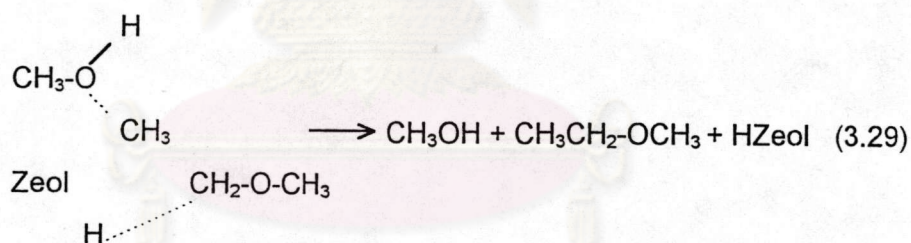
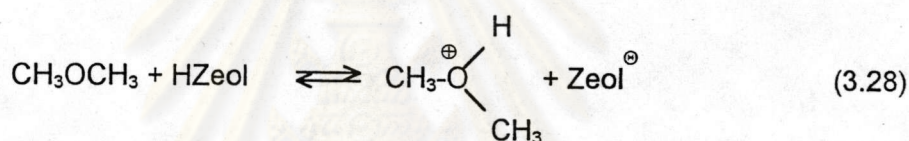
Figure 3.23 Arrhenius plot of the dimethyl ether conversion on zeolite H-ZSM-5 [59]. $P_x = 50.7 \text{ kPa}$; $WHSV = 0.72 \text{ h}^{-1}$

It should be noted that ylid mechanisms have been earlier proposed to explain C-C bond formation from organic N and S compounds in the presence of zeolites. One such example is the formation of stilbene from benzyl mercaptan over Na13X reported by Venuto and Landis [60]. Although these workers preferred an α -elimination mechanism for this reaction, they recognized that a sulfonium ylid

contains an electron-withdrawing group, reaction with diazomethane occurs, as in the following reaction reported by Maerwein et al. [63]:

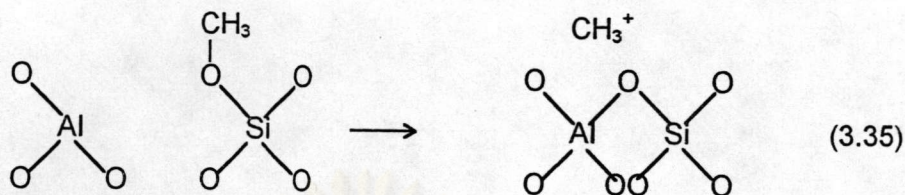


Methanol conversion over phosphorus-modified ZSM-5 was studied by Kaeding and Butter, who proposed the following mechanism based also on oxonium intermediates:



The key step in this mechanism is the labilization of a C-H bond, assisted by anionic sites in the zeolite. The resultant nucleophilic species then attacks the "incipient methyl carbonium ion" from protonated methyl ether (or methanol).

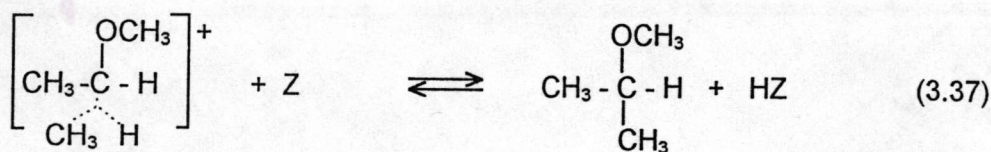
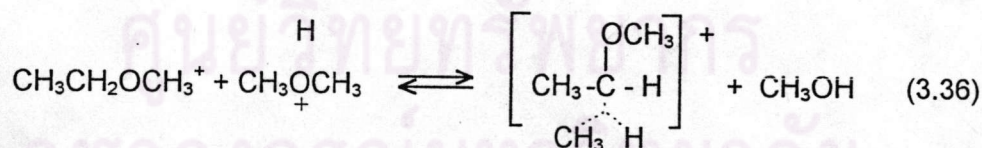
Generation of the methyl cation was considered to occur by polarization of surface methoxyl species:



Autocatalysis involving condensation of methanol and olefins was cited as the reason why little methane is produced via hydride abstraction.

Ono et al. rejected the possibility of carbene involvement. They found that HCl did not poison the methanol reaction over HZSM-5. They reasoned that since HCl poisons base-catalyzed reactions, basic sites do not participate in the reaction. They assert that these results "plead against the carbene mechanism, in which the abstraction of a proton from a methyl group by basic sites is essential."

The Olah superacid mechanism was also favored by Kagi [66], who proposed a series of oxonium intermediates, e.g.,



However, Chang considered the bulky transition states arising from such reactions improbable in ZSM-5 on account of limitations due to channel size.

It should be noted that neither CH_3^+ nor CH_2^+ have thus far been directly observed in superacid solutions. It has also been pointed out that SbF_5 and SO_3 are strong oxidizing species and could generate carbeniumions from alkanes by oxidation, although Olah points out that similar carbocation transformation are observed in systems such as HF-TaF_5 and HF-BF_3 which have high redox potentials, and therefore would not be potent oxidizing media.

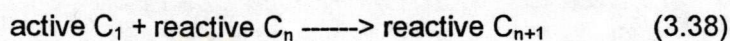
Salem [67] has reported the conversion of methanol and dimethyl ether to hydrocarbons over TaF_5 and NbF_5 At 300°C in an autoclave, a twofold excess of methanol was converted to a mixture of paraffins and aromatics. The NbF_5 -catalyzed reaction gave more light hydrocarbons (>81% $\text{C}_1\text{-C}_5$) than the TaF_5 reaction (53% $\text{C}_1\text{-C}_5$). It was not clear whether the TaF_5 and NbF_5 were stable to hydrolysis under the reaction conditions or deactivated during the course of reaction.

The conversion of methanol over the alkylammonium zeolite Nu-1 was investigated by Spencer and Whittam [68]. They concluded that strong acidity is needed for the fast initial step and that cationic intermediates are involved. However, neither CH_3^+ nor oxonium ions were considered to be plausible.

3.8.2.5 Chain Mechanisms

Anderson et al., using deuterium labeling, found that in the methylation of benzene with methanol over HZSM-5 at 207°C , there is no exchange involving methyl hydrogens. From this it was inferred that in the methanol-to hydrocarbon reaction, the initial step does not involve lability of the C-H bond prior to C-C bond

formation, and that therefore the reactive intermediates are not carbene, carbonic, or oxymethylene species. Instead, a active C_1 entity of the type $(CH_3)RO^+H$ ($R = H$ or CH_3) was proposed, which participates in a chain propagation mechanism



where C_n is an olefin. This is a highly attractive scheme in that it is consistent with the observed autocatalysis of the reaction. In such a scheme, moreover, the precise nature of the C_1 species becomes somewhat of a moot question. However, as has been noted, the temperature at which these D-labeling experiments were carried out was below the threshold for hydrocarbon formation from methanol in the presence of ZSM-5. Thus their bearing on the mechanistic question may be somewhat tenuous. The results of Matsushima and White[69] on deuterium exchange between CH_3OH and CD_3OD over alumina have already been mentioned. It will be recalled that these authors found little D-exchange between CH_3OH and CD_3OD over alumina have already been mentioned. It will be recalled that these authors found little D-exchange below $237^\circ C$ but complete scrambling at higher temperature ($T \geq 397^\circ C$)

ศูนย์วิทยทรัพยากร
จุฬาลงกรณ์มหาวิทยาลัย